Trimethylsilylcellulose/Polystyrene Blends as a Means To Construct Cellulose Domains on Cellulose

Eero Kontturi,† Peter C. Thüne,* and J. W. (Hans) Niemantsverdriet

Schuit Institute of Catalysis, Eindhoven University of Technology, P.O. Box 513, 5600 MB Eindhoven, The Netherlands

Received March 2, 2005; Revised Manuscript Received September 26, 2005

ABSTRACT: A method to prepare films of conspicuous domains of cellulose on a closed cellulose layer is introduced. These films can be used as model surfaces which are closer to the natural environment than most organic model surfaces that are usually coated directly on an inorganic substrate. The method is based on spin-coating a hydrophobic derivative of cellulose, trimethylsilylcellulose (TMSC), blended with polystyrene (PS) onto a silicon substrate. TMSC can be hydrolyzed to cellulose with acid hydrolysis, leaving domains of cellulose and PS embedded on a sublayer of cellulose. Selective dissolving of PS leaves a closed cellulose surface (sublayer) with eminent cellulose domains whose size depends on the original TMSC/PS ratio. The chemistry of the films was analyzed with X-ray photoelectron spectroscopy (XPS) and the morphology with atomic force microscopy (AFM). Scrutiny of the AFM data showed that the films are quantifiable and quantitatively reproducible.

1. Introduction

As the most abundant biopolymer, cellulose has a broad range of industrial applications, ranging from papermaking and textiles to membranes and biomass gasification. Therefore, it is particularly attractive for fundamental research purposes. Although relatively simple in molecular structure, cellulose has proved to be a surprisingly challenging subject of research. The supramolecular structure of various crystalline forms of cellulose was under debate for nearly a century, and despite the recent breakthroughs with synchrotron X-ray and neutron diffraction,[1−3] much remains unknown, such as the nature of amorphous cellulose[4,5] and its supramolecular rearrangements during wetting and drying.[6,7]

Native cellulose is usually included in a cell−wall matrix like wood fiber. It means that other compounds, like lignin and hemicellulose, are embedded in cellulose and that they cannot be removed without altering the structure and morphology of native cellulose. In addition to the complexity of several crystalline forms as well as the amorphous form, each individual cell is—as a product of nature—different in morphology and chemical composition. Under these circumstances, a need for a representative model is evident.

Smooth, ultrathin model surfaces of well-defined substances provide a means to observe the chemical and morphological changes in various conditions which often resemble industrial processes. The amount of fundamental information that can be extracted from model surfaces is already widely recognized in polymer science.[8−14] Cellulose is a tricky substance from the point of view of model surface preparation because of its immiscibility to common solvents.[15] However, there are published methods to prepare cellulose model surfaces by Langmuir−Blodgett deposition,[16−18] spin-coating,[19−21] and casting an emulsion of water in oil on a substrate.[22]

Scheme 1. Hydrolysis of Trimethylsilylcellulose (TMSC) to Cellulose

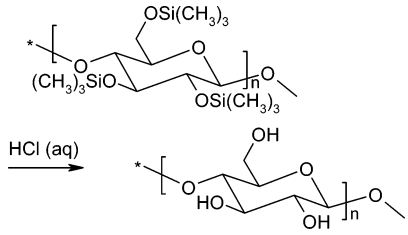

Our group has contributed a novel, fast, and reproducible method to prepare model surfaces of cellulose.[23,24] The method is based on using a dissolving derivative trimethylsilylcellulose (TMSC), spin-coating the TMSC from solution as a thin film on a smooth substrate, and subsequently hydrolyzing the TMSC to cellulose by vapor phase acid hydrolysis on the substrate, leaving a smooth, ultrathin film of cellulose (Scheme 1). In this paper, we want to refine the aforedescribed method to create a cellulose model surface with a completely unprecedented morphology, that of conspicuous, micrometer-scale cellulose domains on a continuous, closed layer of cellulose. The novel morphology is obtained by exploiting polymer blends of TMSC and polystyrene (PS).

Binary polymer blends have been subject to extensive research since the 1970s, and their bulk properties, both physical and chemical, are thus well exposed.[25−28] The tendency for phase separation (spinodal decomposition) of different polymers is so great that even deuterated polymers can separate from their protonated counterparts.[26,27] The different phases have usually a disordered, isotropic morphology.[27,28] This phase separation is decisively altered in the presence of a surface because of the surface forces and the geometrical constraints.[29,30] Roughly two kinds of separation behaviors can be addressed. Vertical separation arises in films which, for example, express thermodynamic equilibrium: the component with lower surface energy is enriched on the

† Currently in: Laboratory of Forest Products Chemistry, Helsinki University of Technology, P.O. Box 6300, 02015 TKK, Finland.

* Corresponding author: e-mail p.c.thuene@tue.nl; Ph +31 40 247 3081; Fax +31 40 247 3481.

10.1021/ma0504419 CCC: $30.25
Published on Web 12/02/2005

surface.[31−33] The other case is lateral separation which takes place especially during rapid solvent evaporation: because of a complex interplay of polymer−solvent, polymer−polymer, and polymer−substrate interactions, the resulting film shows lateral separation to two types of phases with a morphology which, at times, appears aesthetically eccentric.[34−47] Simulations have suggested that the morphology is a result of a competition between diffusive and hydrodynamic growth.[48] Vertical and lateral separation are not mutually exclusive cases; in fact, often both are found within the films.[34,46,47] Moreover, rapid casting of the film does not necessarily mean lateral phase separation since lamellar structures have been observed in spin-cast blend films.[34,49] To summarize, the choice of solvent, compatibility of polymers, and varying the blend composition and the concentration (viscosity) significantly affect the subsequent morphology of binary polymer blend films.[34,36,38,40−42,46,47]

Besides the effect of various coating parameters to their morphology and composition, the polymer blend films have been applied to study dewetting in binary systems.[34,38,41,50,51] In addition, there are accounts of tailoring specific kinds of surfaces with the aid of polymer blends.[39,45,51,52] With this paper, we want to bring our contribution to the latter application.

The hydrolysis of trimethylsilylcellulose (TMSC) to cellulose marks a transformation of a relatively hydrophobic structure to a hydrophilic one (Scheme 1).[24] If one considers mixing TMSC with another hydrophobic polymer and hydrolyzing the TMSC to cellulose after spin-coating the mixture, a binary polymer blend film with a hydrophobic and hydrophilic component emerges. We chose polystyrene (PS) as the hydrophobic polymer to be blended with TMSC.

The cellulose/PS films alone are of interest to the growing applications of polymer films in, for instance, microelectronics, lubrication, sensors, medicine, or bioengineering.[30] It is clear from the earlier references[29−52] that polymer blend films have been extensively scrutinized, and therefore we want to focus on another aspect of exploiting the cellulose/PS films: we will demonstrate how the selective dissolving of the PS phase in the film will lead to a cellulose surface that actually has conspicuous domains of cellulose on a flat layer of cellulose. The eminent cellulose domains with their distinct morphology offer a better possibility to track down the morphological changes during treatments than the previously established flat films[16−24] which are more suitable for, for instance, surface force and adsorption studies. These surfaces also overcome a limitation of organic model surfaces: that the Young's modulus and thermal expansion coefficient of the model substance are totally different to those of the inorganic substrate, which can lead to rupture or delamination upon harsh treatments.[50,53−55] Moreover, as cellulose in its native environment is often embedded with various other forms of cellulose (amorphous vs crystalline), different polysaccharides, and lignin, we take the model surfaces of cellulose one step closer to the natural state of cellulose.

2. Experimental Section

Materials. Trimethylsilylcellulose (TMSC) was prepared from microcrystalline cellulose (Aldrich, DP ∼ 150) and characterized with XPS and ATR-IR as described previously.[23,24] The degree of substitution of the TMSC was 2.3 (2.3 out of 3 hydroxyls in cellulose replaced by TMS groups). Toluene was p.a. grade from Merck. Polystyrene was the secondary standard grade from Aldrich; typical molecular weight according to the manufacturer was 280 000 Da.

Preparation of Model Surfaces. 10 g/L solutions in toluene were prepared from both TMSC and polystyrene (PS). The joint solutions of TMSC and PS were prepared by mixing the two 10 g/L solutions and diluting the rest with toluene in such a fashion that the concentration of the major component was 5.0 g/L and the minor component 2.5 g/L. Thus, in the spin-coating solution of TMSC:PS 1:2, the concentration of TMSC was 2.5 g/L, and the concentration of polystyrene was 5.0 g/L. In TMSC:PS 2:1 solution, the ratios were inverse.

The solutions were spin-coated with a spinning speed of 4000 revolutions per minute (rpm). The substrates used were untreated silicon wafers (Topsil) with (100) surface orientation, cut to ca. 2×2 cm^2 squares.

The regeneration of the spin-coated TMSC to cellulose was performed by acid hydrolysis. A small amount of 2 M hydrochloric acid was placed on the bottom of a glass container with a holder for the spin-coated wafers. The vapor pressure was allowed to stabilize for an hour, after which the wafer was placed in the container and the vapor phase acid hydrolysis was carried out for 2 min.

The PS phase of hydrolyzed cellulose/PS films was dissolved by immersing the sample in toluene for 1 h in 65 °C under magnetic stirring. After the immersion the wafer was removed from the solute, rinsed several times with fresh toluene, also heated to 65 °C, and dried in laboratory air. The hot toluene quickly evaporated from the hydrophilic cellulose surface.

Atomic Force Microscopy (AFM). AFM was performed with Solver P47H base with a SMENA head, manufactured by NT-MDT. The cantilever of choice was contact silicon CSC12 manufactured by Micromasch, used in tapping mode. The typical force constant of the cantilever was in the region of 2.0 N/m and the typical resonance frequency around 150 kHz. The radius of curvature for the tip was always less than 10 nm, according to the manufacturer. Free oscillating amplitude of the cantilever was ∼10 nm, and the set point amplitude was set close (∼70%) to the free-oscillating amplitude in order to work in the regime where long-range attractive forces dominate the amplitude reduction. This gave the best topographic information and minimized the sample indentation.[56,57] All measurements were performed at room temperature.

X-ray Photoelectron Spectroscopy (XPS). XPS was performed using VG Escalab 200 system with an aluminum anode (Al Kα = 1486.3 eV) operating at 510 W with a background pressure of 2×10^{-9} mbar. The spectra were recorded with 20 eV pass energy, 0.1 eV step, and 0.1 s dwell time. The angle between the X-ray beam and the surface normal was kept at 0° unless otherwise mentioned. Using synthetic Gaussian−Lorentzian (30−70) peaks, the C 1s spectra were resolved into different contributions of bonded carbon that are known to exist in the cellulose and TMSC molecules, namely C−O, O−C−O, C−Si, and C−H_X. The normal charge correction by setting the saturated carbon peak (C−H_X) to 285.0 eV was not applicable because the saturated carbon stemmed from different origins (polystyrene and hydrocarbon impurities), and their binding energies are thus not exactly similar. In consequence, the spectra were charge corrected by setting the C−O (hydroxyl) contribution to 286.7 eV. The chemical shifts were obtained from the literature.[58] The exact applied values were −1.7 eV (C−H_X from impurities), −2.0 eV (C−H_X from polystyrene), −2.2 eV (C−Si), +1.4 eV (O−C−O), +2.7 eV (O−C=O), and +5.8 eV (shake-up).

3. Results and Discussion

Morphology by AFM. The AFM image of spin-coated film of TMSC/PS blend with a ratio 2:1 is presented in Figure 1a, indicating heavily a case of lateral phase separation. Two separate domains are visible in amplitude images, but their height difference is unremarkable, as illustrated by a representative height scan below the image. The height distribution

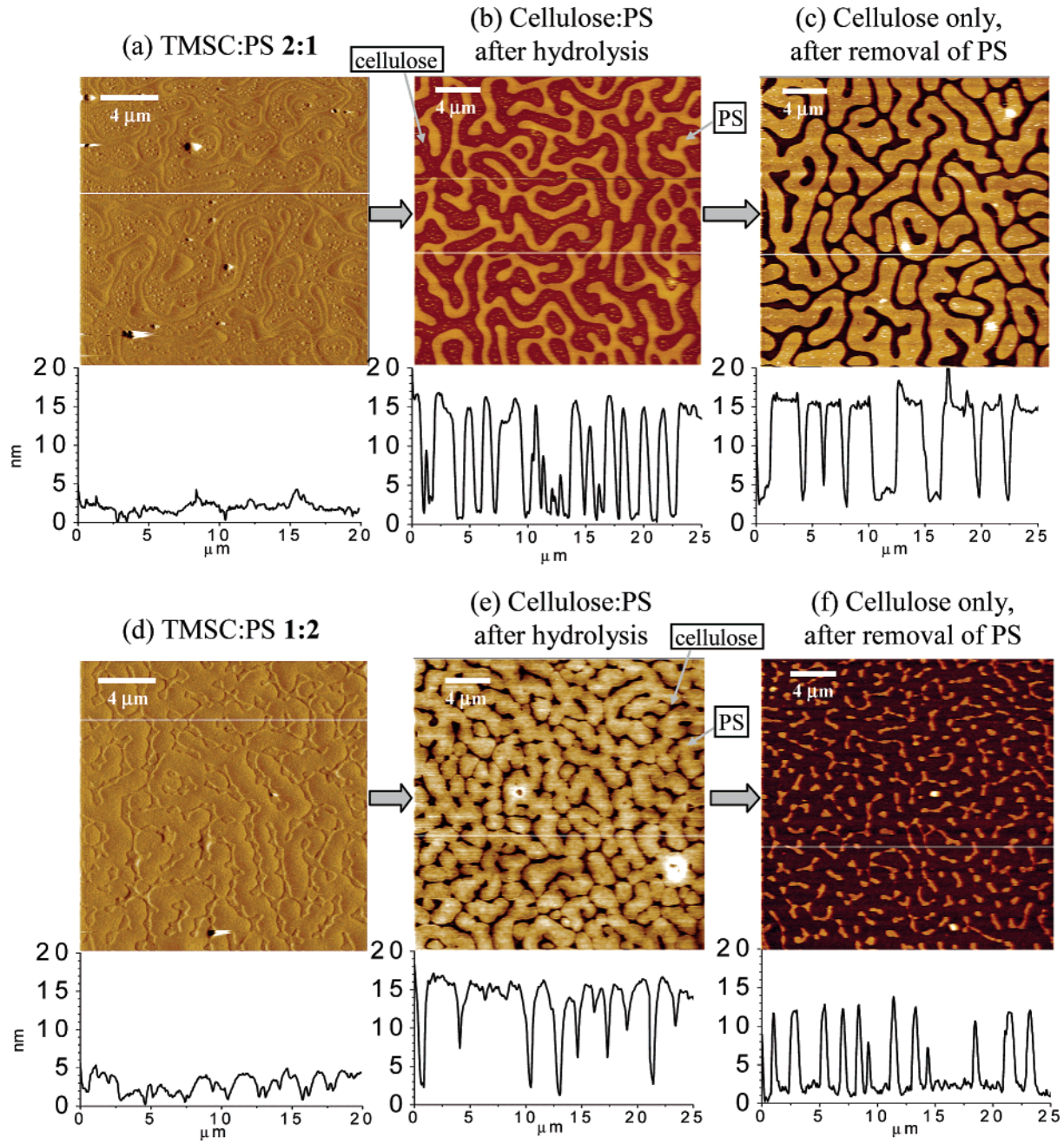

Figure 1. 25 × 25 μm^2 AFM scans from (a) TMSC/PS spin-coated with a ratio 2:1; (b) same film with TMSC hydrolyzed to cellulose; (c) same film, polystyrene has been removed leaving only cellulose on the surface; (d) TMSC/PS spin-coated with a ratio 1:2; (e) same film with TMSC hydrolyzed to cellulose; (f) same film, polystyrene has been removed leaving only cellulose on the surface. (a) and (d) are amplitude images; (b), (c), (e), and (f) are height images. A representative height scan is provided underneath every image. A line in the image indicates the position of that height scan.

histogram (not shown) did not indicate a presence of two separate height regimes. After the hydrolysis of the TMSC to cellulose, the separation of phases is apparent: as the bulky TMSC contracts significantly by the hydrolysis to a concise cellulose structure, the phases can be identified as shown in Figure 1b. The brighter regions are the polystyrene which remains unchanged in an acid environment whereas the darker regions represent the cellulose which has sunk in during the hydrolysis due to the loss of bulky TMS groups and the tight hydrogen-bonding network of cellulose. This distinction is further illustrated in Figure 1c where the surface has been immersed in toluene (65 °C) for 1 h with magnetic stirring. Toluene selectively dissolves the polystyrene, leaving the cellulose unchanged on the surface. Thus, the darker regions in Figure 1c represent what used to be polystyrene, and out of this phase islandlike cellulose domains protrude. The cellulose islands have an approximate width of 2−3 μm, length of 2−15 μm, and a height of 12 nm.

An inverse ratio of TMSC/PS blend to that of Figure 1a is used to produce the film depicted in Figure 1d (TMSC/PS = 1:2). Again, the height separation of the two domains is meager in Figure 1d, although they are visible in the amplitude image. However, upon hydrolysis of TMSC to cellulose, the separation becomes distinct in height (Figure 1e). The cellulose sinks in and appears as the lower (darker) regions, and the polystyrene remains the higher, continuous phase surrounding the cellulose features. The larger PS ratio naturally ac-

counts for a larger amount of polystyrene than in Figure 1b. Toluene immersion exposes fully the cellulose (Figure 1f), previously confined by the large PS phase. The resulting film consists of cellulose domains with a width of ca. 1 μm, length of 2−4 μm, and an average height of about 10 nm. As the preparation conditions for the two films in Figures 1a−c and 1d−f are the same except for the TMSC/PS ratio, the effect of the polymer ratio to the morphology is strikingly evident.

From the cellulose/PS films of Figure 1b,e we can conclude that inverse TMSC/PS ratios lead to somewhat inverted morphologies. The nearly bicontinuous cellulose phase in Figure 1b is replaced by the continuous PS phase of Figure 1e. Thus, by altering the TMSC/PS ratios from 2:1 to 1:2, we get two cellulose surfaces with different, yet distinct, morphologies (Figure 1c,f).

Besides the major lateral phase separation, smaller incompatible domains exist in the films of Figure 1, especially in the TMSC and cellulose phases of TMSC:PS 2:1 sample (Figure 1a,b). This kind of "secondary phase separation" has been scrutinized in simulations: when the hydrodynamic flow is too fast for the diffusion to establish a local equilibrium, geometrical coarsening takes place and secondary phase separation takes place.[48,59] In our system, there is constant diffusion of PS throughout the spin-coating process from the TMSC-rich phase to the PS-rich phase (and vice versa, but the TMSC diffusion from PS-rich phase is much faster because of the higher mobility of the TMSC). As the solvent evaporates rapidly due to the hydrodynamic quench of spin-coating and the phases become more viscous, the diffusion of the PS becomes slower. Eventually polystyrene concentrates on the smaller domains of Figure 1a,b when the attraction between the PS molecules becomes higher than the driving force for the decreasing diffusion.

Chemical Composition by XPS. The chemical composition of the TMSC/PS blends was characterized by XPS. Figure 2 shows the corresponding deconvoluted C 1s spectra to the images in Figure 1, that is, the TMSC/PS ratios of 2:1 and 1:2 (Figure 1a,d) and the subsequent hydrolysis of TMSC to cellulose (Figure 1b,e) and PS removal with toluene (Figure 1c,f). Parts a and d of Figure 2 show the untreated films of TMSC/PS of ratios 2:1 and 1:2, respectively. The O−C−O and C−O contributions stem solely from TMSC, and their ratio (0.21−0.23) is in agreement with the atomic ratios within the TMSC (or cellulose), which is theoretically 0.2. The C−H_X contribution originates from polystyrene and the C−Si ratio from the TMS groups of the TMSC. Additional to C−H_X, PS also contributes to the shake-up peak from the energy loss of the photoelectrons from the aromatic carbons.[60] The difference between the binding energies of the C−H_X and C−Si contributions differs by less than 0.5 eV. Therefore, one should treat this distinction with care. It is nevertheless apparent that the larger PS share with TMSC/PS 2:1 ratio (Figure 2d) ends up as a higher C−H_X contribution than with the lower PS ratio (Figure 2a).

Hydrolysis of TMSC to cellulose changes the chemistry of the film decisively as the C−Si contribution disappears, and the deconvolution is more distinct (Figure 2b,e). Peaks attributed to polystyrene (C−H_X and shake-up) have a higher share from the C 1s area than the TMSC/PS ratio would imply, especially with the lower TMSC (now cellulose) concentration (Figure 2e). Cellulose is much smaller in size than TMSC, owing

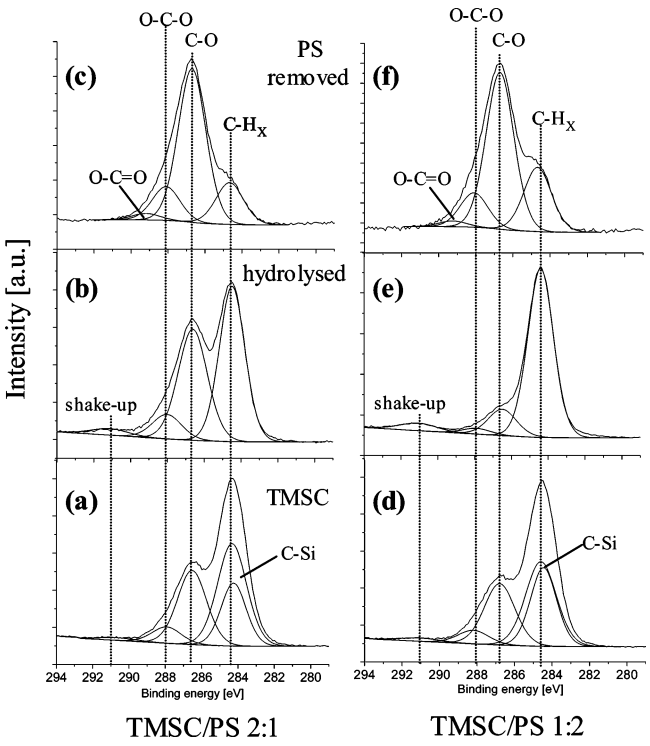

Figure 2. C 1s bands from the XPS spectra: (a) TMSC/PS spin-coated with a ratio 2:1; (b) same film with TMSC hydrolyzed to cellulose; (c) same film, polystyrene has been removed leaving only cellulose on the surface; (d) TMSC/PS spin-coated with a ratio 1:2; (e) same film with TMSC hydrolyzed to cellulose; (f) same film, polystyrene has been removed leaving only cellulose on the surface.

to the concise hydrogen-bonding network and the absence of the bulky TMS groups, but this is not the only explanation. The larger than expected share of PS related can be explained by the fact that carbon contributes to only 6/11 of the atoms in cellulose whereas polystyrene has only carbon within the atoms detectable by XPS (i.e., excluding hydrogen). Taking the atomic ratios into account, the corrected cellulose/PS ratios are 61/39 for the original 2:1 ratio and 25/75 for the original 1:2 ratio. Polystyrene still retains a predominance over cellulose with respect to the ratios, but one must bear in mind that the original TMSC/PS ratios are based on weight percentages. This gives polystyrene (M = 104 g mol^{-1}/monomer) a molar advantage over TMSC (M = 328 g mol^{-1}/monomer for 2.3 degree of substitution). More importantly, the omnipresent hydrocarbon contaminations[60] add up to the C−H_X contribution.

The removal of polystyrene shows up as a considerable decrease in the C−H_X contribution and a loss of the shake-up peak (Figure 2c,f). However, the C−H_X contribution has still a large share in the both C 1s spectra, and the C−H_X peak is much larger than in the corresponding C 1s spectra of the smooth, closed films.[24] The size of the C−H_X contribution, moreover, is in correlation with the original amount of PS in the spin-coating mixture. An additional point of concern is that, upon the removal of PS, a new peak emerges in the C 1s spectrum: a carboxylic (O−C=O) contribution (Figure 2c,f). Since all the data presented here are reproducible, we can only conclude that the PS removal leaves impurities on the surface. The toluene used to dissolve the polystyrene is the same grade as used for the spin-coating so it is very unlikely to contribute for the impurities. In consequence, the polystyrene itself

Table 1. Average Heights of the Protruding PS Domains before PS Dissolution and Cellulose Domains after PS Dissolution (from Height Distribution Histograms of the AFM Images)[a]

original ratio	height of protruding PS [nm]	height of cellulose domains [nm]	total height of PS (Σ) [nm]	thickness of the cellulose sublayer [nm]
TMSC/PS 2:1	13.5 ± 0.5 (Figure 1b)	11.5 ± 0.5 (Figure 1c)	25 ± 1	5 ± 1
TMSC/PS 1:2	13.5 ± 0.5 (Figure 1e)	10 ± 0.5 (Figure 1f)	23.5 ± 1	3.5 ± 1

[a] Total heights of PS domains are calculated by adding up the heights of PS and cellulose domains. Cellulose sublayer is calculated from the scratched images of Figure 4.

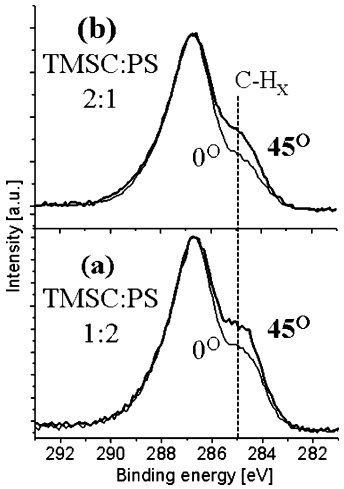

Figure 3. Angle-resolved XPS spectra. 0° is the standard angle between the analyzer and the surface normal; 45° renders the analysis more surface sensitive: (a) cellulose film from TMSC/PS 1:2, hydrolyzed and PS removed; (b) cellulose film from TMSC/PS 2:1, hydrolyzed and PS removed.

must be the source of the impurities visible in Figure 2c,f. The carboxylic contribution does not appear in the cellulose/PS films (Figure 2b,e) because of the high amount of polystyrene on the surface. Dissolving the polystyrene enriches the trace impurities, formerly *in* the polystyrene, to the film surface, and XPS detects them because of its high surface sensitivity. Remnants of polystyrene are very unlikely to contribute to the impurities because of the absence of the shake-up peak. A fatty acid is a candidate for the impurity by containing both C−H$_X$ and carboxylic carbons and not being soluble in toluene. Angle-resolved XPS with 45° angle instead of the normal 0° between the analyzer and the surface normal of the sample was trialed, making the analysis more surface sensitive.[60] The C−H$_X$ contribution showed a growing tendency, indicating that the impurities are, indeed, on the surface (Figure 3). The carboxylic contribution is too small to show visually detectable change.

As for the XPS wide scans of the samples (not shown), no unexpected elements were discovered on the surface. The peaks detected were carbon, oxygen, and a small amount of silicon (except for the unhydrolyzed TMSC where the silicon peak was large). In the case of samples where PS has been removed, the silicon peak stems from the silicon substrate, not, for instance, from the possible remnants of unhydrolyzed TMSC. As reliably expressed in our earlier work,[24] the hydrolysis from TMSC to cellulose is complete with even shorter exposures than presently used.

From the chemical survey by XPS, we can conclude that the method of spin-coating TMSC with polystyrene results in a layer of both compounds. The (complete) hydrolysis of TMSC results in a cellulose layer, blended with polystyrene, with C−O/O−C−O ratio in correlation with theoretical value of cellulose (Table 1). The selective dissolving of polystyrene by toluene leaves a cellulose surface with some impurities, possibly fatty acids. These impurities are enriched on the surface.

Quantitative Survey. The question to arise from Figure 1 and the XPS data is: are the cellulose domains in Figure 1d,f embedded on the silicon substrate, or is there a closed layer of cellulose between the domains and the silicon? And if there is a sublayer of cellulose underneath the domains, how thick is this layer? From the studies with polystyrene/poly(methyl methacrylate) blends we know that, with a favorable choice of solvent and substrate, the more polar poly(methyl methacrylate) forms a continuous layer between the phase segregated structures and the substrate when a more polar substrate like gold or silicon oxide is used.[34] Since the degree of substitution of the TMSC is 2.3, on average 0.7 hydroxyl groups prevail per one monomer of TMSC. These hydroxyl groups, together with the heterocyclic ring structure, make TMSC far more polar than PS. Thus, a layer of TMSC and, subsequently, cellulose is to be expected between the segregated cellulose/PS structures and a silicon substrate. This sublayer of cellulose would imply that we have, indeed, conspicuous domains of cellulose on a closed layer of cellulose after the polystyrene has been removed.

The low silicon contribution in the XPS spectra and the baseline in the height scan of Figure 1f already indicate that the cellulose domains are lying on a surface which is rougher than the expected ±3 Å variation on a surface of a silicon wafer. Figure 4 shows a closer (1×1 μm^2) scan of the surface in Figure 1f, i.e., the cellulose after removal of polystyrene. The scan is taken from a "connection" point of two higher cellulose domains. It is evident from Figure 4a that both the domains and the background consist of similar, grain-like structures which bear a candid resemblance to the closed cellulose films.[23,24] Scratching the surface is a common method to gain information from the AFM figures, and it has been utilized also with polymer blends.[61] Here the scratching unambiguously reveals the presence of the sublayer for the cellulose surface prepared from TMSC/PS ratio 1:2 (Figure 4b). The flat silicon surface is exposed underneath the sublayer of cellulose. The thickness of the sublayer is ca. 3−4 nm. Figure 4c shows a scratched cellulose surface prepared from TMSC/PS ratio of 2:1. The cellulose sublayer here is rougher than in Figure 4b; its thickness is 4−6 nm.

As for the formation of the sublayer, it has been proposed that a transient bilayer is formed because preference of the other polymer toward the substrate favors the asymmetric segregation but that this bilayer then becomes unstable and dewetting of the upper surface occurs. The holes in the upper phase are then filled by the lower phase.[62,63] Sprenger et al. speculated on two different instabilities during spin-coating of binary blends: one caused by increasing unfavorable enthalpic interactions as the solvent concentration decreases and one named instability of the free surface caused by, for example, hydrodynamic instability.[47] The

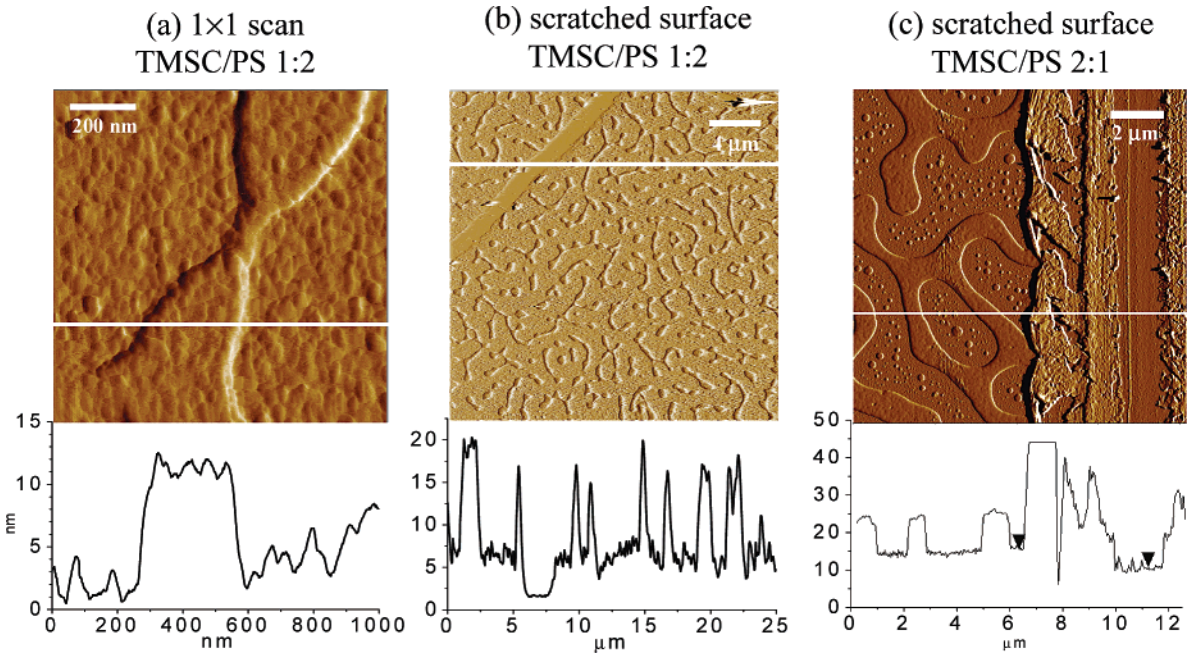

Figure 4. (a) $1 \times 1\ \mu m^2$ AFM scan of cellulose on cellulose sample, originally from TMSC/PS 1:2, hydrolyzed and PS removed; (b) $25 \times 25\ \mu m^2$ AFM scan of a scratched cellulose on cellulose sample, originally from TMSC/PS 1:2, hydrolyzed and PS removed; (c) $12 \times 12\ \mu m^2$ AFM scan of a scratched cellulose on cellulose sample, originally from TMSC/PS 2:1, hydrolyzed and PS removed. All images are amplitude images. The representative height scan underneath the images is indicated with a white line in each image.

Table 2. Relative Areas of Cellulose and Polystyrene on the Surface of the Cellulose/PS Samples As Determined from AFM Height Distributions and from the XPS Data, and the Apparent Height of Cellulose in Cellulose Only Films[a]

original ratio	AFM (cellulose/PS)[b]	AFM (cellulose only)[b]	XPS (cellulose/PS)[c]	apparent height of cellulose [nm][d]
TMSC/PS 2:1	59/41 (Figure 1b)	66/34 (Figure 1c)	61/39 (Figure 2b)	12.6 (Figure 1c)
TMSC/PS 1:2	35/65 (Figure 1e)	15/85 (Figure 1f)	25/75 (Figure 2e)	5.0 (Figure 1f)

[a] The cellulose/PS ratio in the AFM (cellulose only) column is calculated with the assumption that the cellulose sublayer used to be filled with polystyrene. The corresponding figure, from which the calculation has been made, is expressed in parentheses. The errors are deduced from analyses of parallel samples. [b] Error ±1. [c] Error ±2. [d] The apparent height is calculated by adding the sublayer and the domains corrected by their coverage in cellulose only films.

former leads to phase separation on a length scale of a few micrometers whereas the latter leads to undulations of a few tens of micrometers. The films presented in this paper represent the smaller scale phase separation only. The dewetting scheme has received further support from Jukes et al., who followed spin-coating of a binary blend in situ with time-resolved light scattering.[64]

AFM height images actually yield three-dimensional information which has recently been exploited with integral-geometry approach for polymer blends.[65] Also, simpler methods exist for AFM data analysis, and we have utilized a straightforward histogram analysis, elaborated for polymer blends by Affrossman et al.[61] The histograms in this work showed a two-peak distribution in the height count histograms, corresponding to cellulose phase (lower) and PS phase (higher), in the case of cellulose/PS blends. The distance between the peaks yielded the height of the protruding PS phase. In a similar fashion, the height distribution histograms of cellulose only films were examined. The peaks correspond to the cellulose sublayer (lower) and the protruding cellulose domains (higher). The total height of the PS phase was calculated by adding the heights of the protruding PS phase in the cellulose/PS film and protruding cellulose phase in the cellulose only films. (The space between the cellulose domains used to be polystyrene before it was removed.) When these results are combined with the thickness of the cellulose sublayers, we get the full map of the vertical dimensions of the films,[61] tabulated to Table 1. The errors are calculated from the variations between five parallel samples.

It is also possible to yield the coverage of the PS and cellulose domains from the height distribution histograms by comparing the areas of the PS and cellulose peaks.[61] Table 2 expresses the relative areas taken by each component in the AFM scan. First, the height distributions of images from cellulose/PS films are calculated, corresponding to Figure 1b,e. Then the relative amounts of the cellulose sublayer and the cellulose domains are calculated, and the area of the cellulose sublayer is attributed to polystyrene because it used to be polystyrene before it was removed with toluene. The cellulose/PS ratios from the XPS data (from Figure 2) are also presented in Table 2.

At first glance, the surprising element in Table 2 is the low amount of cellulose in the films originating from the TMSC/PS 1:2 ratio: the apparent height of the 1:2 ratio is only 40% of that of 2:1 ratio. From previous studies, however, we know that the thickness of the TMCS and subsequent cellulose layer grows by the factor of 2.5 when the TMSC spin-coating concentration is doubled.[24] This is in correlation with the apparent heights of cellulose in Table 2.

In addition, Table 2 shows apparent nonuniformity of the cellulose/PS ratios in the TMSC/PS 1:2 sample

Scheme 2. (a) TMSC/PS Blend; (b) TMSC Is Hydrolyzed to Cellulose and the Phase Contracts; (c) PS Is Removed by Selective Dissolution with Toluene, Leaving a Closed Cellulose Surface with Conspicuous Domains of Cellulose Protruding from It

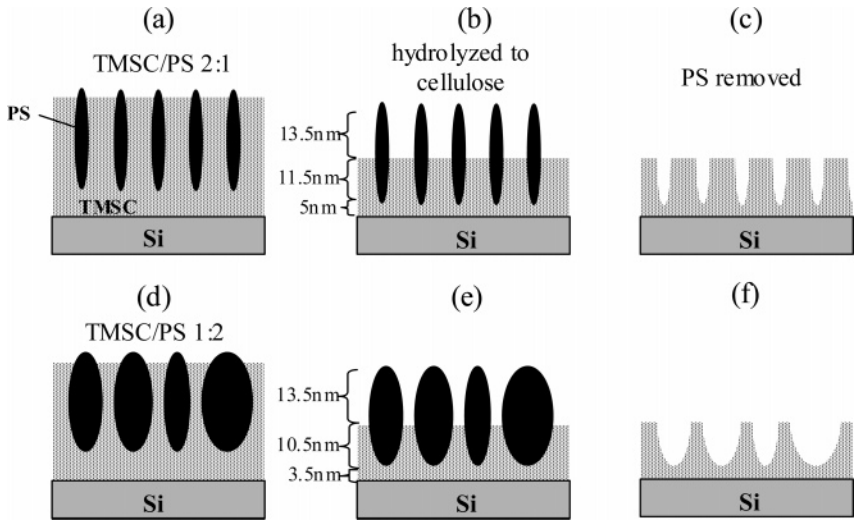

AFM from cellulose/PS and cellulose only films, and the XPS data show different values. We propose that this lack of coherence in the data lies in the dropletlike shape of the polystyrene. In other words, the vertical borderline between the lateral PS and TMSC phases is initially curved so that PS appears as dropletlike structures because of its lower surface tension.[34] This gives PS phase an apparent dominance in the cellulose/PS films of the TMSC/PS 1:2 ratio (Table 2). There is curvature in the TMSC/PS 2:1 films as well, but the larger size of the cellulose domains subdues the effect on the cellulose/PS ratio and the figures of the TMSC/PS 2:1 sample are much more in correlation with each other (Table 2). We have to emphasize that this is merely a proposition. The parabola-shaped features of polystyrene (Figure 1b,e) and cellulose (Figure 1c,f) after PS removal, however, advocate that the PS is in a dropletlike shape in these films.

The differences in XPS and AFM data of TMSC/PS 1:2 sample are probably caused by both the dropletlike structure of PS phase and hydrocarbon impurities which contribute to a seemingly larger amount of polystyrene (Table 2). Moreover, the sampling depth of XPS is no more than 10 nm, and the most of the data are received from the first few nanometers, which means that not all the cellulose is probed by the XPS, especially the cellulose in the sublayer.

The ambiguity of the figures in Table 2 shows that AFM and XPS have to be used with the selective dissolving of the other polymer in order to gain more reliable results. Different spin-coating parameters, such as speed, solvent, and solution concentration, as well as diverse TMSC/PS ratios would undoubtedly reveal more about the complex interplay between the components during the rapid solvent removal of the spin-coating process. However, advanced treatise of the interactions between TMSC, PS, substrate, and solvent is beyond the scope of this introduction. Our aim here has been to demonstrate that the hitherto unknown cellulose on cellulose films are feasible and that there are ways to quantify the films with histogram analysis from the AFM scans and scratching of the cellulose sublayer. We must emphasize, furthermore, that the data represented are completely reproducible as witnessed by the five parallel samples for each stage of the analyses; i.e., there is little or no ambiguity in the morphology of the films themselves. It is apparent, therefore, that the cellulose on cellulose films provide a viable, quantitative template for further studies on cellulose.

Finally, a schematic, cross-sectional representation of the preparation with the quantified data is shown in Scheme 2. During spin-coating, a thin TMSC layer is formed on the substrate surface as the lateral phase separation of TMSC and PS takes place on top of that layer (a). The TMSC layer contracts upon its transformation to cellulose during hydrolysis, leaving the PS layer protruding from a sea of cellulose (b). The lateral size of the PS domains depends on the TMSC/PS ratio. As the PS is removed by toluene immersion, the remaining cellulose structure is left intact, resulting in domains of cellulose lying on a continuous sublayer of cellulose (c). The droplet shape of the PS phase is exaggerated, but it illustrates clearly why the dropletlike structure affects the TMSC/PS 1:2 ratio more because of the smaller size of the cellulose domains—hence the ambiguity in cellulose/PS ratios in Table 2.

4. Conclusions

We describe the formation of a new kind of cellulose film which can be used as a model surface. The preparation takes place in three steps: (i) blending trimethylsilylcellulose (TMSC) and polystyrene (PS) in a toluene solution and spin-coating the mixture on a silicon wafer; (ii) hydrolyzing the TMSC to cellulose after the spin-coating; (iii) dissolving the polystyrene which leaves cellulose intact on the surface.

The resulting surfaces consist of conspicuous domains of cellulose on a cellulose sublayer (cellulose on cellulose). The thickness of the sublayer and the size of the cellulose domains are depended on the TMSC/PS ratio in the spin-coating process. The TMSC/PS 2:1 ratio results in a cellulose sublayer of 4−6 nm and 66% coverage of cellulose domains with an approximate width of 2−3 μm, length of 2−15 μm, and a height of 11.5 nm. TMSC/PS 1:2 ratio results in a 3−4 nm cellulose sublayer and 15% coverage of cellulose domains with a width of ca. 0.4−1.0 μm, length of 2−4 μm, and an average height of 10 nm. The chemical

composition of these films was characterized with X-ray photoelectron spectroscopy (XPS), which showed that the films consisted of cellulose with a slight impurity on the surface. The surface impurity is likely to be a fatty acid.

The AFM height data were scrutinized in height distribution histograms and compared with the XPS data. This quantitative survey revealed nonuniformity in the cellulose/PS ratio of the TMSC/PS 1:2 samples with respect to the analytical method used. This nonuniformity was concluded to stem from the dropletlike shape of the PS domains. The sample with an original TMSC/PS 2:1 ratio had more uniform figures because of the much smaller size of the PS domains where the curvature of the dropletlike shape is likely to have a belittled effect. Despite the minor discrepancies within the quantitative analyses, the data were completely reproducible: five parallel samples gave very similar figures in repeated experiments. The reproducibility of the films *and* the quantitative data are encouraging concerning the further applications of these films.

The cellulose on cellulose films are a novel and important introduction to the literature of cellulose model surfaces. There is inevitably a demand for diverse cellulose model surfaces because of the unparalleled natural and industrial importance of cellulose. Fundamental applications of these films may consist of, for instance, investigating supramolecular rearrangements of cellulose during wetting and subsequent drying (papermaking, recycling) or chemical and morphological changes upon heat treatment (biomass gasification). The closed, thin sublayer of cellulose offers a unique advantage that takes these films closer to the natural environment of cellulose where it is incorporated in a matrix of various other forms of cellulose and other carbohydrates. The conspicuous domains allow interpretations based on the morphology in contrast to the previously established smooth cellulose model surfaces. Furthermore, the morphology can be quantified with a histogram analysis of the AFM scans, which provides data with hard numbers in addition to the qualitative images. The huge chemical and physical difference of an inorganic substrate and organic cellulose is also overcome with these surfaces as the cellulose domains are embedded on a substrate of their own chemical and physical nature. The trace impurity on the surface is a nuisance. On the other hand, as the natural fibers are always covered by the surface-enriched hydrocarbon extractives,[66] a fatty acid on the surface of these films can be considered, euphemistically, again a step closer to authenticity.

Acknowledgment. The research described is part of the project "Fibre raw material technology for sustainable production of paper and board". This project is one of the activities of the Dutch Centre of Competence Paper and Board and is supported by the Dutch Ministry of Economic Affairs. They are acknowledged for their financial support.

References and Notes

(1) Nishiyama, Y.; Sugiyama, J.; Chanzy, H.; Langan, P. *J. Am. Chem. Soc.* **2003**, *125*, 14300.
(2) Nishiyama, Y.; Langan, P.; Chanzy, H. *J. Am. Chem. Soc.* **2002**, *124*, 9074.
(3) Langan, P.; Nishiyama, Y.; Chanzy, H. *Biomacromolecules* **2001**, *2*, 410.
(4) Paakkari, T.; Serimaa, R.; Fink, H.-P. *Acta Polym.* **1989**, *40*, 731.
(5) O'Sullivan, A. C. *Cellulose* **1997**, *4*, 173.
(6) Scallan, A. M.; Tigerström, A. C. *J. Pulp Pap. Sci.* **1992**, *18*, 188.
(7) Newman, R. H. *Cellulose* **2004**, *11*, 45.
(8) Sheiko, S. S.; Gauthier, M.; Möller, M. *Macromolecules* **1997**, *30*, 2343.
(9) Valignat, M. P.; Oshanin, G.; Villette, S.; Cazabat, A. M.; Moreau, M. *Phys. Rev. Lett.* **1998**, *80*, 5377.
(10) Reiter, G.; Sharma, A.; Casoli, A.; David, M.-O.; Khanna, R.; Auroy, P. *Langmuir* **1999**, *15*, 2551.
(11) Loos, J.; Thüne, P. C.; Niemantsverdriet, J. W.; Lemstra, P. J. *Macromolecules* **1999**, *32*, 8910.
(12) Sheiko, S. S. *Adv. Polym. Sci.* **2000**, *151*, 61.
(13) Luzinov, I.; Julthongpiput, D.; Bloom, P. D.; Sheares, V. V.; Tsuruk, V. V. *Macromol. Symp.* **2001**, *166*, 227.
(14) Vogt, B. D.; Soles, C. L.; Jones, R. L.; Wang, C.-Y.; Lin, E. K.; Wu, W.-I.; Satija, S. K.; Goldfarb, D. L.; Angelopoulos, M. *Langmuir* **2004**, *20*, 5285.
(15) Klemm, D.; Philipp, B.; Heinze, T.; Heinze, U.; Wagenknecht, W. *Comprehensive Cellulose Chemistry*; Wiley-VCH: Weinheim, 1998; Vol. 1, Chapter 2.
(16) Schaub, M.; Wenz, G.; Wegner, G.; Stein, A.; Klemm, D. *Adv. Mater.* **1993**, *5*, 919.
(17) Buchholz, V.; Wegner, G.; Stemme, S.; Ödberg, L. *Adv. Mater.* **1996**, *8*, 399.
(18) Holmberg, M.; Wigren, R.; Erlandsson, R.; Claesson, P. M. *J. Colloid Interface Sci.* **1997**, *186*, 369.
(19) Gunnars, S.; Wågberg, L.; Cohen Stuart, M. A. *Cellulose* **2002**, *9*, 239.
(20) Fält, S.; Wågberg, L.; Vesterlind, E.-L.; Larsson, P. T. *Cellulose* **2004**, *11*, 151.
(21) Edgar, C. D.; Gray, D. G. *Cellulose* **2003**, *10*, 299.
(22) Kasai, W.; Kondo, T. *Macromol. Biosci.* **2004**, *4*, 17.
(23) Kontturi, E.; Thüne, P. C.; Niemantsverdriet, J. W. *Polymer* **2003**, *44*, 3621.
(24) Kontturi, E.; Thüne, P. C.; Niemantsverdriet, J. W. *Langmuir* **2003**, *19*, 5735.
(25) Vasile, C. In *Handbook of Polymer Blends and Composites*; Vasile, C., Kulshreshtha, A. K., Eds.; Rapra Technology Limited: Shawbury, 2003; Vol. 3A, Chapter 3.
(26) Bates, F. S.; Wignall, G. D.; Koehler, W. C. *Phys. Rev. Lett.* **1985**, *55*, 2425.
(27) Bates, F. S.; Muthukumar, M.; Wignall, G. D.; Fetters, L. J. *J. Chem. Phys.* **1988**, *89*, 535.
(28) Snyder, H. L.; Meakin, P. *J. Chem. Phys.* **1983**, *79*, 5588.
(29) Jones, R. A. L.; Norton, L. J.; Kramer, E. J.; Bates, F. S.; Wiltzius, P. *Phys. Rev. Lett.* **1991**, *66*, 1326.
(30) Budkowski, A. *Adv. Polym. Sci.* **1999**, *148*, 1.
(31) Jones, R. A. L.; Kramer, E. J.; Rafailovich, M. H.; Sokolov, J.; Schwarz, S. A. *Phys. Rev. Lett.* **1989**, *62*, 280.
(32) Chiou, J. S.; Barlow, J. W.; Paul, D. R. *J. Polym. Sci., Part B: Polym. Phys.* **1987**, *25*, 1459.
(33) Lhoest, J. B.; Bertrand, P.; Weng, L. T.; Dewez, J. L. *Macromolecules* **1995**, *28*, 4631.
(34) Walheim, S.; Böltau, M.; Mlynek, J.; Krausch, G.; Steiner, U. *Macromolecules* **1997**, *30*, 4995.
(35) Böltau, M.; Walheim, S.; Mlynek, J.; Krausch, G.; Steiner, U. *Nature (London)* **1998**, *391*, 877.
(36) Tanaka, K.; Takahara, A.; Kajiyama, T. *Macromolecules* **1996**, *29*, 3232.
(37) Bar, G.; Thomann, Y.; Brandsch, R.; Cantow, H.-J. *Langmuir* **1997**, *13*, 3807.
(38) Tanaka, K.; Takahara, A.; Kajiyama, T. *Macromolecules* **1998**, *31*, 863.
(39) Walheim, S.; Schäffer, E.; Mlynek, J.; Steiner, U. *Science* **1999**, *283*, 520.
(40) Müller-Buschbaum, P.; Gutmann, J. S.; Stamm, M. *Macromolecules* **2000**, *33*, 4886.
(41) Müller-Buschbaum, P.; Gutmann, J. S.; Wolkenhauer, M.; Kraus, J.; Stamm. M.; Smilgies, D.; Petry, W. *Macromolecules* **2001**, *34*, 1369.
(42) Busch, P.; Posselt, D.; Smilgies, D.-M.; Rheinländer, B.; Kremer, F.; Papadakis, C. M. *Macromolecules* **2003**, *36*, 8717.
(43) Chen, C.; Wang, J.; Woodcock, S.; Chen, Z. *Langmuir* **2002**, *18*, 1302.
(44) Spanos, C. G.; Ebbens, S. J.; Badyal, J. P. S.; Goodwin, A. J.; Merlin, P. J. *Macromolecules* **2003**, *36*, 368.
(45) Ngwa, W.; Wannemacher, R.; Grill, W.; Serghei, A.; Kremer, F.; Kundu, T. *Macromolecules* **2004**, *37*, 1691.
(46) Ton-That, C.; Shard, A. G.; Teare, D. O. H.; Bradley, R. H. *Polymer* **2001**, *42*, 1121.

(47) Sprenger, M.; Walheim, S.; Budkowski, A.; Steiner, U. *Interface Sci.* **2003**, *11*, 225.
(48) Wagner, A. J.; Yeomans, J. M. *Phys. Rev. Lett.* **1998**, *80*, 1429.
(49) Geoghegan, M.; Jones, R. A. L.; Payne, R. S.; Sakellariou, P.; Clough, A. S.; Penfold, J. *Polymer* **1994**, *35*, 2019.
(50) Wang, P.; Koberstein, J. T. *Macromolecules* **2004**, *37*, 5671.
(51) Tong, Y. J.; Huang, X. D.; Chung, T. S. *Macromolecules* **2001**, *34*, 5748.
(52) Gan, D.; Shiqiang, L.; Cao, W. W. *Eur. Polym. J.* **2004**, *40*, 2481.
(53) Iyer, K. S.; Luzinov, I. *Langmuir* **2003**, *19*, 118.
(54) Bouchet, J.; Roche, A. A.; Hamelin, P. *Thin Solid Films* **1999**, *355*−*356*, 270.
(55) Coupeau, C.; Naud, J. F.; Cleymand, F.; Goudeau, P.; Grilhé, J. *Thin Solid Films* **1999**, *353*, 194.
(56) San Paulo, A.; García, R. *Biophys. J.* **2000**, *78*, 1599.
(57) García, R.; San Paulo, A. *Phys. Rev. B* **1999**, *60*, 4961.
(58) Beamson, G.; Briggs, D. *High-Resolution XPS of Organic Polymers;* John Wiley & Sons: Chichester, 1992.
(59) Tanaka, H.; Araki, T. *Phys. Rev. Lett.* **1998**, *81*, 389.
(60) Niemantsverdriet, J. W. *Spectroscopy in Catalysis*, 2nd ed.; Wiley-VCH: Weinheim, 2000; Chapter 3.
(61) Affrossman, S.; Stamm, M. *Colloid Polym. Sci.* **2000**, *278*, 888.
(62) Ton-That, C.; Shard, A. G.; Bradley, R. H. *Polymer* **2002**, *43*, 4973.
(63) Raczkowska, J.; Bernasik, A.; Budkowski, A.; Sajewicz, K.; Penc, B.; Lekki, J.; Lekka, M.; Rysz, J.; Kowalski, K.; Czuba, P. *Macromolecules* **2004**, *37*, 7308.
(64) Jukes, P. C.; Heriot, S. Y.; Sharp, J. S.; Jones, R. A. L. *Macromolecules* **2005**, *38*, 2030.
(65) Raczkowska, J.; Rysz, J.; Budkowski, A.; Lekki, J.; Lekka, M.; Bernasik, A.; Kowalski, K.; Czuba, P. *Macromolecules* **2003**, *36*, 2419.
(66) Laine, J.; Stenius, P.; Carlsson, G.; Ström, G. *Cellulose* **1994**, *1*, 145.

MA0504419